2011 Drucker Medal Paper: Localized Compaction in Porous Sandstones

J. W. Rudnicki
Professor
Fellow ASME
Departments of Civil and Environmental Engineering and Mechanical Engineering,
Northwestern University,
Evanston, IL 60201
e-mail: jwrudn@northwestern.edu

Compaction bands are narrow, roughly planar zones of localized deformation, in which the shear is less than or comparable to compaction. Although there are differences in their appearance in the field and in laboratory specimens, they have been observed in both for high-porosity (greater than about 15%) sandstones. Because the porosity in them is reduced and the tortuosity increased, they inhibit fluid flow perpendicular to their plane. Consequently, they can alter patterns of fluid movement in formations in which they occur and are relevant to applications involving fluid injection or withdrawal. Formation of compaction bands is predicted by a framework that treats localized deformation as a bifurcation from homogeneous deformation. This paper gives a brief overview of compaction localization but focuses on field and laboratory observations that constrain two parameters entering the bifurcation analysis: a friction coefficient μ and a dilatancy factor β. The inferred values suggest that normality ($\mu = \beta$) is not satisfied, and compaction localization occurs on a transitional portion of the yield surface, where the local slope in a plot of Mises equivalent shear stress versus compressive mean normal stress changes from positive ($\mu > 0$) to negative ($\mu < 0$). These inferences are at odds with critical state and cap theories that typically assume normality and predict dilation on the portion of the surface where $\mu > 0$. In addition, the values suggest that the critical state ($\mu = 0$) does not necessarily correspond to zero volume change.
[DOI: 10.1115/1.4025176]

1 Introduction

This paper is based on the content of the Drucker Medal Lecture, entitled "Formation and Extension of Compaction Bands in Porous Sandstone," presented at the ASME Winter Annual Meeting in Denver, Nov. 2011. This written version is only a brief summary of the material covered in the oral presentation. It is neither a complete description of research on compaction bands nor does it cite all relevant work on compaction bands. Nevertheless, the papers that are cited do offer a reasonable entree into the literature. The paper does present two comparisons of observation with a bifurcation theory of band formation that have not appeared elsewhere.

The outline follows the organization of the oral version: (i) What are compaction bands?; (ii) Why are they important?; (iii) What do they look like?; (iv) Why do they form?; (v) How do they propagate?; and (vi) What are some open questions?

2 What Are Compaction Bands?

Although field observations initially stimulated interest in compaction bands, they are easiest to illustrate in terms of the most common testing configuration for rock deformation: axisymmetric compression, shown schematically in Fig. 1. A cylinder of rock is loaded hydrostatically to a desired pressure. Thereafter, the confining pressure on the lateral surfaces remains constant and the axial stress is increased, usually until failure. For small axial load increases, the deformation remains relatively homogeneous, although there is inevitably some inhomogeneity due to constraint at the ends of the specimen. This is illustrated in Fig. 1(*b*), in which the distance between the horizontal lines is reduced uniformly from Fig. 1(*a*). Further increase of the axial load causes this more or less homogeneous pattern of deformation to give way to localized deformation in a narrow, roughly planar band (Fig. 1(*c*)), at least if the confining stress and temperature are not too high. For low-porosity (less than about 5%) rocks, the deformation in the band is predominantly shear accompanied by some dilation. Typically, the normal to the band makes an angle on the order of 55–65 degrees with the specimen axis. Recently, however, there has been increasing attention on failure in more porous rocks (15%–25%), in which the normal to the band is nearly perpendicular to the specimen axis and the deformation in the band is predominantly compaction (Fig. 1(*d*)). These are compaction bands, and the porosity in the band can be reduced 10%–15% from that in the host rock. Although pure compaction bands (essentially no shear) have been identified in the field, more common are bands for which the deformation is a combination of

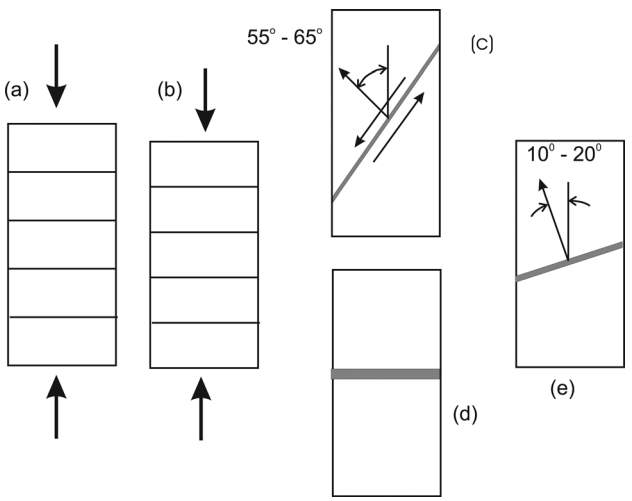

Fig. 1 Schematic illustration of localized band formation in the axisymmetric compression test

Manuscript received June 26, 2013; final manuscript received July 31, 2013; accepted manuscript posted August 2, 2013; published online September 6, 2013. Editor: Yonggang Huang.

compaction with a lesser or equal amount of shear. In these cases, the normal to the band is about 10–20 degrees from the specimen axis (Fig. 1(*e*)).

3 Why Are Compaction Bands Important?

The significance of compaction bands both with and without shear is that they reduce the porosity and increase the tortuosity [1] relative to the host material. Consequently, they reduce the permeability for flow across the bands from one to several orders of magnitude. Because the bands have been identified in rock types and formations that are often host for fluids, their presence can significantly alter the flow characteristics of the formations. These fluids may be naturally occurring, as in oil, gas, and water, and it is desired to withdraw them. Or they may be the result of injection, for example, of natural gas for storage or of CO_2 for sequestration to prevent its emission to the atmosphere and the accompanying deleterious effects on climate. In either case, deformation naturally or by operations of injection and withdrawal may cause the formation of these bands. Because these bands are narrow, less than 1 cm, they are difficult to detect by geophysical methods from the surface or from borehole observations. Consequently, it is important to understand the conditions for their formation and propagation.

4 What Do Compaction Bands Look Like?

Compaction bands were first reported in the field by Ref. [2] in the Aztec Sandstone in Valley of Fire State Park, Nevada, but they attracted more attention when the term was applied by Ref. [3] to structures in the Navajo Sandstone in Utah. Additional, observations have been reported by Ref. [4] in Utah and by Refs. [5–7] in Nevada. Recently, Ref. [8] reported observations from Provence, France. Pure compaction bands, involving a minimal amount of shear, do occur but are less common than bands with comparable amounts of both shear and compaction.

Although the bands are roughly planar, they occur in a variety of configurations with varying thicknesses, spacings, waviness, and orientations. Band thicknesses are roughly the order of 1 mm–1 cm, and lengths can range from tens of centimeters to a few meters. Porosity within the bands is reduced by fracturing and rearrangement of grains, but crushing of grains is generally not observed.

Compaction bands have also been observed in axisymmetric compression tests in the laboratory (see, e.g., Refs. [9–11]). Typically, bands initiate near the ends of specimens, presumably triggered by the inhomogeneity there. As the load increases, bands spread toward the center of the specimen, leaving a laminated structure of very compacted and less compacted material. Bands are roughly planar but have an undulating appearance on the microscale, perhaps indicating that locally they are not pure compaction bands but a combination of shear and compaction. Bands are narrow, only a few grains in width. A different pattern of compaction has been observed in one rock, Castlegate Sandstone. Compaction progressed as a front from the ends of the specimen rather than forming a banded structure [12]. In contrast to bands observed in the field, those in laboratory specimens exhibit severe grain crushing. In addition, formation of bands in the laboratory require much higher stress levels than thought to be present when bands formed in the field.

Successive formation of bands in the laboratory is often associated with a burst of acoustic emission and a small stress drop (see, e.g., Ref. [9]). The stress strain curve is qualitatively similar to that observed in crushing of honeycombed material (see, e.g., Fig. 2 in Ref. [13]), but strains in the honeycomb are much larger and the micromechanics are completely different. In the honeycomb material, the small stress drops correspond to collapse of a layer of cells triggered by buckling of a cell wall. A comparable triggering mechanism has not been identified for porous sandstones.

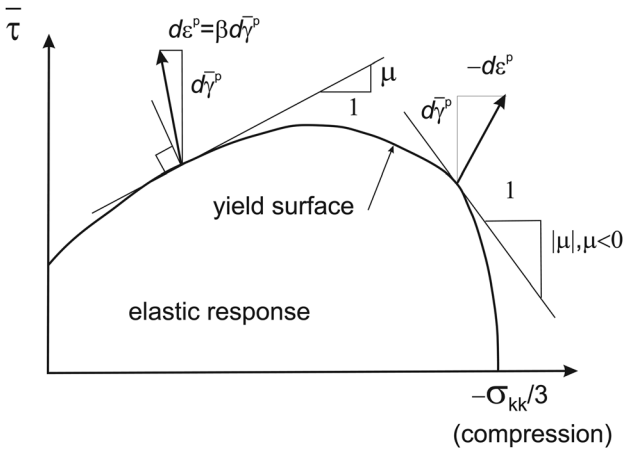

Fig. 2 Schematic illustration of a yield surface for a high-porosity sandstone

There have been suggestions for reconciling the differences between the bands observed in the field and the laboratory [11], but these differences are not thoroughly understood. Nevertheless, the phenomena seem sufficiently similar that their formation is related and a better understanding of compaction formation under the more controlled conditions of the laboratory will contribute to understanding their formation in the field.

5 Why Do the Bands Form?

Phenomenological behavior of materials in which compaction bands form is roughly consistent with a framework that treats localization as a bifurcation from homogeneous deformation [14–16]. These analyses are based on rate-independent elastic-plastic constitutive relations. Although there are results for more complex material models, the analyses of Ref. [14] (and Ref. [15]) are for a material with yield surface and plastic potential that depend only on the mean stress ($\sigma_{kk}/3$, positive in tension) and the Mises equivalent shear stress ($\bar{\tau} = (\sigma'_{ij}\sigma'_{ij}/2)^{1/2}$, where σ'_{ij} is the deviatoric stress). The dependences of the yield surface and plastic potential on the mean stress are, in general, different (non-normality or nonassociated flow rule). Figure 2 shows a schematic yield surface for the type of material analyzed by Ref. [15]. In addition to the elastic constants (assumed to be isotropic), the constitutive parameters μ and β are illustrated in the figure: μ is the local slope of the yield surface and β is the ratio of inelastic volume strain increment to inelastic equivalent shear strain increment. An additional constitutive parameter is a hardening modulus related to the slope of the stress-strain curve.

For low-porosity rock, only the left side of the surface, where $\mu > 0$ and $\beta > 0$ (dilation), is observed; at higher pressures and/or temperatures, the behavior becomes more ductile, similar to that of a metal. The left side of the surface (referred to as frictional) is also characteristic of higher porosity rocks at relatively low confining pressures. At higher confining pressure, $\mu < 0$ and $\beta < 0$. This portion of the yield surface is often referred to as a cap. It is frequently modeled as an ellipse in rough agreement with data [9,17], but there is an intermediate range, where μ and β have opposite signs (more often with $\mu > 0$ and $\beta < 0$). This is the portion of the yield surface on which compaction localization is often observed.

Figure 2 shows a single smooth surface, but sometimes the frictional and cap portions are treated as two different surfaces. Although there is no direct experimental evidence for this possibility, it is a possible reflection of different micromechanisms that apply in the two regimes. Reference [18] has examined the implications of a two surface model for predictions of the bifurcation theory.

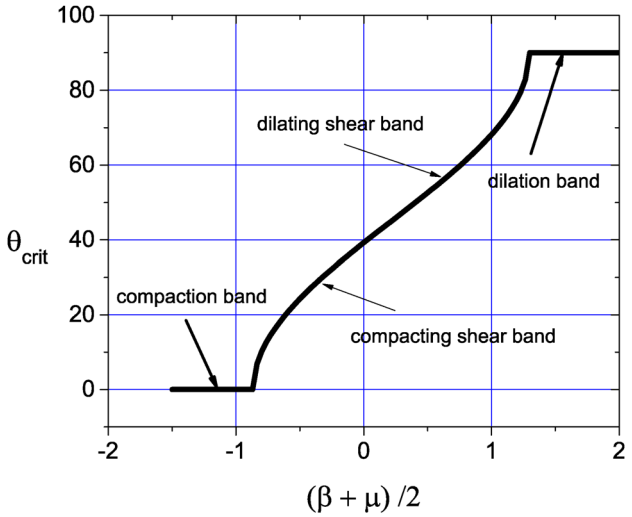

Fig. 3 Predicted variation of the angle between the normal to the plane of localization and the most compressive principal stress against the average of β and μ for axisymmetric compression and Poisson's ratio $\nu = 0.2$

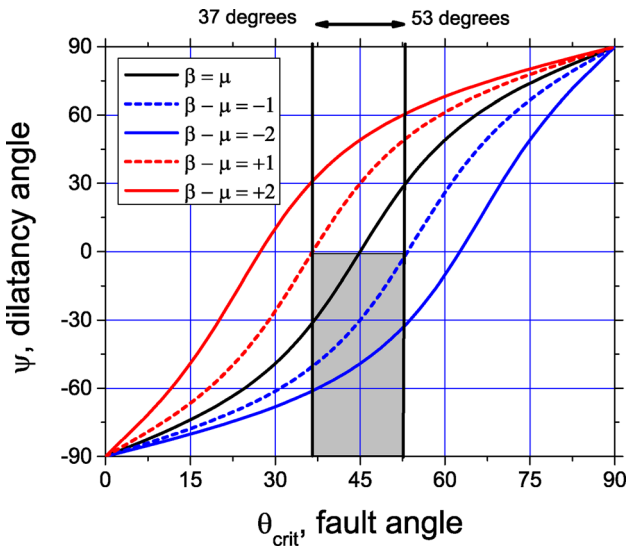

Fig. 4 Dilatancy angle Ψ defined by Ref. [20] against the difference $\beta - \mu$. The shaded rectangle corresponds to compactive localization ($\Psi < 0$) and the range of fault angles, 37–53, reported by Ref. [21] for compacting shear bands in Valley of Fire State Park, Nevada. Modified from Fig. 5.16a of Ref. [16].

Figure 3 plots the band angle (θ_{crit}, angle between the normal to the band of localization and the direction of the most compressive principal stress) predicted from the bifurcation analysis [15,16] against $(\beta + \mu)/2$ for axisymmetric compression. The band angle decreases for decreasing $(\beta + \mu)/2$, reflecting an increasing ratio of compaction to shear in the band (relative to material outside the band). The limiting case of a pure compaction band, a band perpendicular to the maximum compressive stress, occurs for $(\beta + \mu)/2$ sufficiently negative (less than -0.82 in this case). (Observation of the other limiting case of a dilation band that is perpendicular to the least compressive stress has also occasionally been reported [19].) The predicted variation of the band angle and the relative amounts of shear and dilation or compaction are consistent with a change from the frictional to cap portion of the yield surface.

Figure 4 is modified from Fig. 5.16a of Ref. [16]. The vertical axis is the angle defined by Ref. [20]: $\Psi = \arctan(\Delta\varepsilon/\Delta\gamma)$, where

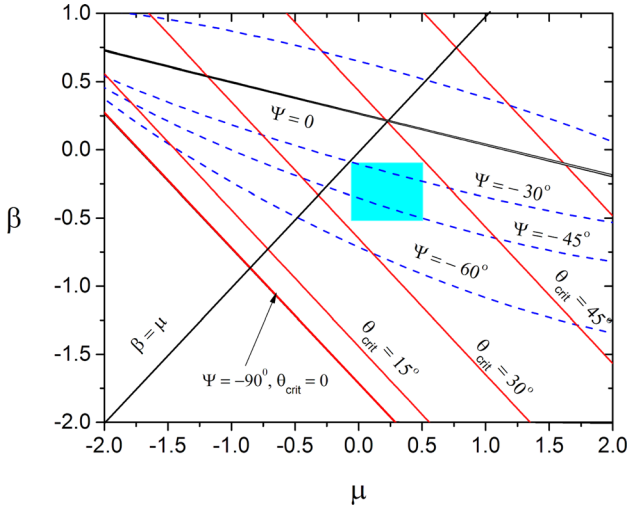

Fig. 5 Modified from Fig. 5.17b of Ref. [16]. Contours of constant dilatancy angle Ψ and fault angle θ_{crit} on a plot of dilatancy factor β against friction coefficient μ. Shaded rectangle shows the range of β and μ for compacting bands from Fig. 9 of Refs. [24,25].

$\Delta\varepsilon$ and $\Delta\gamma$ are the difference between dilation and shear (relative to the band) inside and outside of the band (at formation). Negative values correspond to compaction, and the limiting value of $\Psi = -90$ corresponds to a pure compaction band. Ψ is plotted against the band angle θ_{crit} for different values of the difference $\beta - \mu$, with $\beta = \mu$ corresponding to normality or an associated flow rule. Normality is generally not satisfied for brittle rocks but is often assumed for the cap portion of the yield surface (portion with $\mu < 0$).

The shaded box is for $\Psi \leq 0$, corresponding to compaction, and the range of angles, 37–53 degrees, measured by Ref. [21] for compactive shear bands in the Valley of Fire State Park, Nevada. The measured band angles for compactive shear bands suggest that positive or zero values of $\beta - \mu$ are possible, but there is a wider range of negative values. Since $\beta < 0$ for compaction, $\mu \geq 0$ or $\mu < 0$ with $|\mu| < |\beta|$. Consequently, normality ($\beta = \mu$) is unlikely to apply and the stress state is near the transition from the frictional portion of the surface ($\mu \geq 0$) or barely on the cap (μ slightly less than zero). Both of these features are at odds with critical state models [22] and the cap model [23].

Figure 5 is modified from Fig. 5.17b of Ref. [16]. It shows curves of constant Ψ (dashed) and lines of constant band angle θ_{crit} (solid) on a plot of β versus μ. The shaded rectangle shows the range of β and μ inferred from the laboratory data for four sandstones: Adamswiller, Bentheim, Berea, and Darley Dale, summarized in Ref. [24], Fig. 9 [25]. The rectangle is for samples with localized bands with $\theta_{crit} < 45$ degrees (Ref. [24] refers to these as high angle, because they use the angle between the plane of the band and the maximum compressive stress) that microstructural observations have identified as compactive. The range is small positive values of μ, roughly between 0 and 0.5, and small negative values of β, roughly between -0.5 and 0. These ranges are consistent with the observations of Ref. [21] noted in Fig. 4. These data also indicate that normality is not satisfied and that compaction localization occurs in the transition region of the yield surface.

Reference [24] gives an extensive comparison of its data with the Ref. [26] version of the critical state model [22] and the cap model of Ref. [23]. Although the data roughly agree with the elliptic shape of the yield surfaces for these models, they have several discrepancies with them. The data (and also the inference from the field data of Ref. [21] noted in Fig. 4) suggest that normality is not satisfied, although this is generally assumed for the models. The data also indicate that the critical state does not

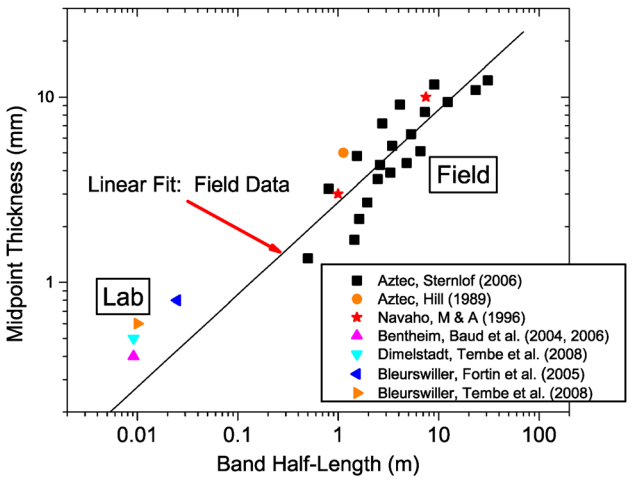

Fig. 6 Compilation of field and laboratory data for midpoint thickness (mm) versus band half-length (m)

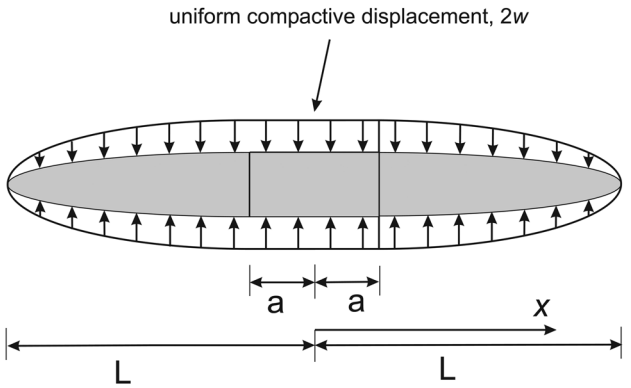

Fig. 7 Schematic of a combined anticrack and antidislocation model for compaction band propagation [27]. Because of the very small aspect ratios of the bands, the actual thickness of the zone (shaded area) is neglected. Consequently, the compactive displacement shown corresponds to interpenetration in the model.

necessarily correspond to no volume change and that compaction is observed on the portion of the surface that predicts dilation in these models.

6 How Do Bands Propagate?

One obvious mechanism for the extension of a compaction band in its own plane is that compaction in the band increases the compressive stress at the edge. Reference [27] explored this possibility by modeling the band as a thin ellipsoidal inhomogeneity with different elastic constants than the surrounding material and subjected to an inelastic compactive strain. The author found that the results were relatively insensitive to the elastic mismatch and, for aspect ratios suggested by field observations [6,28], 10^{-3} to 10^{-4}, the results were essentially indistinguishable from the zero aspect ratio limit. This supported the earlier suggestion of Ref. [29] that compaction bands could be treated as anticracks, that is, tensile cracks with the sign of the stress and displacement reversed. (The concept of an anticrack was introduced by Ref. [30] as a model for pressure solution surfaces.) This predicts interpenetration of the crack surfaces, but the interpenetration is viewed as reflecting inelastic compaction in a narrow band.

Following Refs. [11] and [31], Fig. 6 shows a compilation of field [2,3,28] and laboratory [9,11,24,32] data for midpoint thickness (mm) versus band half-length (m). For low aspect ratios, the midpoint width is a proxy for the compactive displacement. A linear fit to the field data gives

$$2w = AL^B$$

where $B = 0.49891 \approx 0.5$ and $A = 10^{0.43240} \times 10^{-3}$ m$^{1/2}$. This suggests that the midpoint thickness is very nearly proportional to the square root of the band half-length. (Note that, if the band were an anticrack with uniform traction, the midpoint thickness would be proportional to the band length.) Reference [27] proposed a combined anticrack/antidislocation model that has this scaling. The model is shown schematically in Fig. 7; for clarity, it is shown as a finite width zone. Reference [11] has also discussed this model in detail and applied it to the case in which both the field and laboratory bands are assumed to undergo the same inelastic compactive strain. For $|x| \le |a|$, a uniform triggering compactive displacement $2w$ is assumed to occur, causing a stress concentration at $x = \pm L$. A uniform traction is assumed to resist closure on $|a| \le |x| \le |L|$, with magnitude chosen to eliminate the stress singularity at $|x| = |a|$ and ensure that the closure profile is smooth. This is the compactive analog of a tensile crack with a net entrapped dislocation [33].

If $|a| \ll |L|$, then the stress intensity factor is well approximated as

$$K = \sqrt{\frac{\pi}{L}} \frac{\mu w}{(1-\nu)} \tag{1}$$

where μ is the shear modulus and ν is Poisson's ratio. (This is the negative of the usual stress intensity factor, since this is an anticrack.) Using this value in the relation between K and the energy release rate $\mathcal{G} = (1-\nu)K^2/2\mu$ and rearranging yields

$$\frac{2w}{\sqrt{L}} = \sqrt{\frac{8\mathcal{G}(1-\nu)}{\pi\mu}} \tag{2}$$

The magnitude of the triggering compaction is assumed to cause a value of the energy release rate (and also the stress intensity factor) above the critical value for propagation. Because the energy release rate decreases with length, the band grows until it falls below the critical value for propagation. Consequently, the final length reflects this critical value. The position of the laboratory points is above the line in Fig. 6, because the bands in the laboratory traverse the specimen before the energy release rate falls to its critical value.

Using $\mu = 8.33$ GPa and $\nu = 0.2$, values inferred by Ref. [6] for the Valley of Fire, gives a compactive energy release rate of $\mathcal{G} = 30$ kJ/m^2. This is comparable to the value of 40 kJ/m^2 estimated by a modification of method used by Ref. [34] to derive the stress intensity factor for a semi-infinite tensile crack in an infinite layer subjected to rigid displacement boundary conditions. Despite the differences noted earlier between the appearance of bands in the laboratory and field, these values estimated from field observations lie within the range of 4–90 kJ/m^2 estimated by Refs. [35] and [36] from propagation of notched laboratory specimens.

7 What Are Some Open Questions?

Increasing numbers of laboratory and field investigations have provided an improved observational basis for the study of compactive localization, both in the limiting case of pure compaction and when accompanied by shear. There is a rough consistency of observations with theoretical models for band formation and propagation, although the constraints placed upon the theory are weak. There remain numerous significant open questions that must be answered before it is possible to establish a reliable predictive basis.

The differing appearance and stress levels at which bands form in the laboratory and in the field remain an issue. Although there have been attempts to reconcile these differences, it remains surprising that it has not been possible to form compaction bands in the laboratory that are more similar to the bands in the field. One possible reason is that the laboratory experiments have been done on competent sandstones, whereas the bands in the field may have formed in relatively unconsolidated material. Yet compaction bands are seldom observed in laboratory tests on sands unless there is significant grain crushing that is not observed in the field. The grain size distribution and cementation may be factors.

Laboratory results clearly show that water has a weakening effect on strength. Yet effects of the coupling between fluid diffusion and deformation during band formation have not been examined either in theoretical models or laboratory experiments. Field evidence of the effects of water is unclear.

The values of the parameters β and μ inferred from laboratory experiments and, in some cases, from field studies are consistent with bifurcation analyses for compacting shear bands. However, the bifurcation analyses predict much more softening is required for localization than observed. There are many reasons for this but the most prominent is that the constitutive model of Ref. [14], on which most of these predictions are based, is oversimplified. More elaborate models are possible, but these involve parameters that are difficult to determine and constrain by experiment.

The inferred values β and μ also indicate discrepancies with the critical state and cap models, at least as they are usually interpreted. In particular, the assumption of normality typically made in these models is not appropriate and they predict dilation on portions of the yield surface where compaction localization has been observed to occur in the laboratory.

As yet, there is no good physical microstructural model for compaction localization. For example, there is nothing like buckling of the cell wall, which is clearly a trigger for compaction localization in open-cell materials. Presumably, pore collapse, breakage of cementation, and grain crushing are important, but how these are related to a macroscopic constitutive model is not clear. Because experiments indicate that the tendency to develop localized compaction differs in porous rocks of similar porosity, other properties probably play a role. These might include, for example, grain size distribution and secondary constituents.

Anticrack/antidislocation models that attribute propagation of band in its own plane, as driven by a compressive stress concentration, are consistent with available data but are not strongly constrained by it. There is no field evidence for the compactive triggering event that is posited in this model. Even if the initial compaction event is adequately modeled by the bifurcation analysis, there is no comprehensive model for the transition from initiation to full formation and propagation. Indeed, there seems little evidence that has been identified to indicate propagation at all, except for the relative formation times of different sets of deformation bands.

The model of band extension by compressive stress concentration is an appealing one for addressing the growth of an isolated band in its own plane. But bands rarely occur in isolation. Generally, they occur in sets. In the laboratory, the bands typically form sequentially with increasing axial strain. Compaction increases the stiffness of the material, and this provides a plausible reason for lateral propagation. But only in a single rock, Castlegate Sandstone, has lateral propagation as a front been observed (and once the front has propagated through the sample, there is no evidence left of localized compaction). In most other cases, the formation of additional bands leaves relatively uncompacted material between the existing bands. Why does the Castlegate Sandstone behave differently? What controls the spacing of the bands? Do bands in the field form sequentially or simultaneously in sets?

Isolated roughly planar bands do occur in the field, but there is a wide spectrum of other patterns. Bands may vary in thickness, be wavy, and occur in a variety of orientations. Deposition patterns and local stress variations account for some of these features, but there is much that is not well understood.

8 Conclusion

This paper has provided a short overview and introduction to localized compaction in porous sandstones. Material parameters inferred from laboratory and field observations are consistent with a framework that views band formation as a bifurcation from homogenous deformation. But this framework addresses only the formation of a single band, and the evolution of the material behavior that goes into the theory is poorly constrained.

An antidislocation/anticrack model for propagation is consistent with an observed scaling between midpoint width (a proxy for compactive displacement) and band length. But again, observational constraints are weak and the model only addresses the extension of a single band in its own plane. In addition, evidence of the initial compactive event that is assumed to trigger the propagation has not been identified.

Despite considerable progress in observations and modeling compaction bands, there is much that is not understood. There is a particular need for a better understanding of how the micromechanics and secondary constituents are related to macroscopic behavior. Understanding the variety and complexity of field observations remains a formidable challenge.

Acknowledgment

My own work on this topic has been supported primarily by the Geosciences Program of Basic Energy Science in the U.S. Department of Energy. I am also grateful for recent support from the Center for Integrated Petroleum Research, University of Bergen, Norway. I have benefited from numerous conversations over many years with Teng-fong Wong (SUNY Stony Brook and The Chinese University of Hong Kong) and more recently from discussions with Anita Torabi and Elin Skurtveit (Center for Integrated Petroleum Research, University of Bergen, Norway).

References

[1] Sun, W., Andrade, J. E., Rudnicki, J. W., and Eichhubl, P., 2011, "Connecting Microstructural Attributes and Permeability From 3D Topographic Images of In Situ Shear-Enhanced Compaction Bands Using Multiscale Computations," Geophys. Res. Lett., **38**, p. L10302.

[2] Hill, R. E., 1989. "Analysis of Deformation Bands in the Aztec Sandstone, Valley of Fire State Park, Nevada," Master's thesis, University of Nevada, Las Vegas.

[3] Mollema, P., and Antonellini, M. A., 1996, "Compaction Bands: A Structural Analog for Anti-Mode I Cracks in Aeolian Sandstone," Tectonophysics, **267**, pp. 209–228.

[4] Schultz, R. A., 2009, "Scaling and Paleodepth of Compaction Bands, Nevada and Utah," J. Geophys. Res., **114**, p. B03407.

[5] Sternlof, K. R., Chapin, J. R., Pollard, D. D., and Durlofsky, L. J., 2004, "Permeability Effects of Deformation Band Arrays in Sandstone," Am. Assoc. Pet. Geol. Bull., **88**(9), pp. 1315–1329.

[6] Sternlof, K. R., Rudnicki, J. W., and Pollard, D. D., 2005, "Anti-Crack Inclusion Model for Compaction Bands in Sandstone," J. Geophys. Res., **110**, p. B11403.

[7] Aydin, A., and Ahmadov, R., 2009, "Bed-Parallel Compaction Bands in Aeolian Sandstone: Their Identification, Characterization and Implications," Tectonophysics, **479**, pp. 277–284.

[8] Ballas, G., Soliva, R., Sizun, J.-P., Fossen, H., Benedicto, A., and Skurtveit, E., 2013, "Shear-Enhanced Compaction Bands Formed at Shallow Burial Conditions: Implications for Fluid Flow (Provence, France)," J. Struct. Geol., **47**, pp. 3–15.

[9] Baud, P., Klein, E., and Wong, T.-F., 2004, "Compaction Localization in Porous Sandstones: Spatial Evolution of Damage and Acoustic Emission Activity," J. Struct. Geol., **26**, pp. 603–624.

[10] Wong, T.-F., Baud, P., and Klein, E., 2001, "Localized Failure Modes in a Compactant Porous Rock," Geophys. Res. Lett., **28**(13), pp. 2521–2524.

[11] Tembe, S., Baud, P., and Wong, T.-F., 2008, "Stress Conditions for the Propagation of Discrete Compaction Bands in Porous Sandstone," J. Geophys. Res., **113**, p. B09409.

[12] Olsson, W. A., 2001, "Quasistatic Propagation of Compaction Fronts in Porous Rocks," Mech. Mater., **33**, pp. 659–668.

[13] Papka, S. D., and Kyriakides, S., 1998, "Experiments and Full-Scale Numerical Simulations of In-Plane Crushing of a Honeycomb," Acta Metall., **46**(8), pp. 2765–2776.

[14] Rudnicki, J. W., and Rice, J. R., 1975, "Conditions for the Localization of Deformation in Pressure-Sensitive Dilatant Materials," J. Mech. Phys. Solids, **23**, pp. 371–394.
[15] Issen, K. A., and Rudnicki, J. W., 2000, "Conditions for Compaction Bands in Porous Rock," J. Geophys. Res., **105**, pp. 21529–21536.
[16] Bésuelle, P., and Rudnicki, J. W., 2004, "Localization: Shear Bands and Compaction Bands," *Mechanics of Fluid Saturated Rocks* (International Geophysics Series, Vol. 89), Y. Guéguen and M. Boutéca, eds., Academic, New York, pp. 219–321.
[17] Rudnicki, J. W., 2004, "Shear and Compaction Band Formation on an Elliptic Yield Cap," J. Geophys. Res., **109**, p. B03402.
[18] Challa, V., and Issen, K. A., 2004, "Conditions for Compaction Band Formation in Porous Rock Using a Two-Yield Surface Model," J. Eng. Mech., **130**(9), pp. 1089–1097.
[19] Bernard, X. D., Eichhubl, P., and Aydin, A., 2002, "Dilation Bands: A New Form of Localized Failure in Granular Media," Geophys. Res. Lett., **29**(4), p. 2176.
[20] Bésuelle, P., 2001, "Compacting and Dilating Shear Bands in Porous Rock: Theoretical and Experimental Conditions," J. Geophys. Res., **106**(B7), pp. 13435–13442.
[21] Eichhubl, P., Hooker, J. N., and Laubach, S., 2010, "Pure and Shear-Enhanced Compaction Bands in Aztec Sandstone," J. Struct. Geol., **32**, pp. 1873–1886.
[22] Schofield, A. N., and Wroth, P., 1968, *Critical State Soil Mechanics*, McGraw-Hill, New York.
[23] Dimaggio, F. L., and Sandler, I. S., 1971, "Material Model for Granular Soils," J. Engrg. Mech. Div., **97**, pp. 935–950.
[24] Baud, P., Vajdova, V., and Wong, T.-F., 2006, "Shear-Enhanced Compaction and Strain Localization: Inelastic Deformation and Constitutive Modeling of Four Porous Sandstones," J. Geophys. Res., **111**, p. B12401.
[25] Wong, T., 2011, private communication
[26] Carroll, M. M., 1991, "A Critical State Plasticity Theory for Porous Reservoir Rock," *Recent Advances in Mechanics of Structured Continua*, Vol. 117, M. Massoudi and K. R. Rajagopal, eds., Applied Mechanics Division, ASME, New York, pp. 1–8.
[27] Rudnicki, J. W., 2007, "Models for Compaction Band Propagation," Geol. Soc., London, Spec. Pub., **284**, pp. 107–125.
[28] Sternlof, K. R., 2006, "Structural Geology, Propagation Mechanics and Hydraulic Effects of Compaction Bands in Sandstone," Ph.D. thesis, Stanford University, Stanford, CA.
[29] Sternlof, K., and Pollard, D., 2002, "Numerical Modeling of Compactive Deformation Bands as Granular Anti-Cracks," EOS Trans. Am. Geophys. Union, **83**, p. F1347.
[30] Fletcher, R. C., and Pollard, D. D., 1981, "Anticrack Model for Pressure Solution Surfaces," Geology, **9**, pp. 419–424.
[31] Rudnicki, J. W., Tembe, S., and Wong, T.-F., 2006, "Relation Between Width and Length of Compaction Bands in Porous Sandstones," EOS Trans. Am. Geophys. Union, Vol. 87, Fall Meet. Suppl., Abstract T43A-1633.
[32] Fortin, J., Schubnel, A., and Guéguen, Y., 2005, "Elastic Wave Velocities and Permeability Evolution During Compaction of Bleuswiller Sandstone," Int. J. Rock Mech. Min. Sci., **42**(7-8), pp. 873–889.
[33] Rice, J. R., 1968, "Mathematical Analysis in the Mechanics of Fracture," *Fracture: An Advanced Treatise*, Vol. 2, H. Liebowitz, ed., Academic, New York, pp. 191–311.
[34] Rice, J. R., 1968, "A Path Independent Integral and the Approximate Analysis of Strain Concentration by Notches and Cracks," ASME J. Appl. Mech., **35**, pp. 379–386.
[35] Vajdova, V., and Wong, T.-F., 2003, "Incremental Propagation of Discrete Compaction Bands and Microstructural Observations on Circumferentially Notched Samples of Bentheim Sandstone," Geophys. Res. Lett., **30**(14), p. 1775.
[36] Tembe, S., Vajdova, V., Wong, T.-F., and Zhu, W., 2006, "Initiation and Propagation of Strain Localization in Circumferentially Notched Samples of Two Porous Sandstones," J. Geophys. Res., **111**, p. B02409.